International Journal of Pharmaceutics: X 6 (2023) 100197

Contents lists available at ScienceDirect

International Journal of Pharmaceutics: X

journal homepage: www.sciencedirect.com/journal/international-journal-of-pharmaceutics-x

Effect of the amount of cationic lipid used to complex siRNA on the cytotoxicity and proinflammatory activity of siRNA-solid lipid nanoparticles

Mahmoud S. Hanafy [a,c], Huy M. Dao [a], Haiyue Xu [a], John J. Koleng [b], Wedad Sakran [c], Zhengrong Cui [a,*]

[a] Division of Molecular Pharmaceutics and Drug Delivery, College of Pharmacy, The University of Texas at Austin, TX, USA
[b] Via Therapeutics, LLC, Austin, TX, USA
[c] Department of Pharmaceutics, Faculty of Pharmacy, Helwan University, Egypt

ARTICLE INFO

Keywords:
Nanoparticles
Cationic lipid
siRNA
Cytotoxicity
Proinflammatory

ABSTRACT

When preparing siRNA-encapsulated solid lipid nanoparticles (siRNA-SLNs), cationic lipids are commonly included to condense and lipophilize the siRNA and thus increase its encapsulation in the SLNs. Unfortunately, cationic lipids also contribute significantly to the cytotoxicity and proinflammatory activity of the SLNs. Previously, our group developed a TNF-α siRNA-SLN formulation that showed strong activity against rheumatoid arthritis unresponsive to methotrexate in a mouse model. The siRNA-SLNs were composed of lecithin, cholesterol, an acid-sensitive stearoyl polyethylene glycol (2000) conjugate, and siRNA complexes with 1,2-dioleoyl-3trimethylammonium-propane (DOTAP), a cationic lipid. The present study was designed to study the effect of the amount of DOTAP used to complex the siRNA on the cytotoxicity and proinflammatory activity of the resultant siRNA-SLNs. A small library of siRNA-SLNs prepared at various ratios of DOTAP to siRNA (i.e., nitrogen to phosphate (N/P) ratios ranging from 34:1 to 1:1) were prepared and characterized, and the cytotoxicity and proinflammatory activity of selected formulations were evaluated in cell culture. As expected, the siRNA-SLNs prepared at the highest N/P ratio showed the highest cytotoxicity to J774A.1 macrophage cells and reducing the N/P ratio lowered the cytotoxicity of the siRNA-SLNs. Unexpectedly, the cytotoxicity of the siRNA-SLNs reached the lowest at the N/P ratios of 16:1 and 12:1, and further reducing the N/P ratio resulted in siRNA-SLNs with increased cytotoxicity. For example, siRNA-SLNs prepared at the N/P ratio of 1:1 was more cytotoxic than the ones prepared at the N/P ratio 12:1. This finding was confirmed using neutrophils differentiated from mouse MPRO cell line. The DOTAP release from the siRNA-SLNs prepared at the N/P ratio of 1:1 was faster than from the ones prepared at the N/P ratio of 12:1. The siRNA-SLNs prepared at N/P ratios of 12:1 and 1:1 showed comparable proinflammatory activities in both macrophages and neutrophils. Additionally, the TNF-α siRNA-SLNs prepared at the N/P ratios of 12:1 and 1:1 were equally effective in downregulating TNF-α expression in J774A.1 macrophages. In conclusion, it was demonstrated that at least in vitro in cell culture, reducing the amount of cationic lipids used when preparing siRNA-SLNs can generally help reduce the cytotoxicity of the resultant SLNs, but siRNA-SLNs prepared with the lowest N/P ratio are not necessarily the least cytotoxic and proinflammatory.

1. Introduction

Small-interfering RNAs (siRNAs) have received considerable attention for their potential therapeutic applications. To date, the United State Food and Drug Administration (FDA) has approved several siRNA-based products for the treatment of different diseases (Curreri et al., 2022). Solid lipid nanoparticles (SLNs) are commonly used as a delivery vehicle for siRNA in experimental therapy of cancer (Hanafy et al., 2021; Okamoto et al., 2014; Yamamoto et al., 2015), viral infection (Moon et al., 2016; Sato et al., 2017), inflammatory diseases (Aldayel et al., 2018; Zhao et al., 2018), and neurologic disorders (Rungta et al., 2013). Unfortunately, siRNA-SLNs are often not without adverse effects

* Corresponding author.
E-mail address: zhengrong.cui@austin.utexas.edu (Z. Cui).

https://doi.org/10.1016/j.ijpx.2023.100197
Received 22 March 2023; Received in revised form 30 June 2023; Accepted 1 July 2023
Available online 3 July 2023

(Kanasty et al., 2013). The siRNA itself is considered a sequence-dependent potent inducer of inflammatory cytokines in vitro and in vivo (Judge et al., 2005; Robbins et al., 2009). In addition, the lipids in SLNs can be a source of immunogenicity and cytotoxicity, especially the cationic lipids. It was reported that cationic lipids can lead to hepatoxicity, weight loss, T helper type 1 (Th1) and Th17 cytokines, as well as interferon-responsive gene activation (Tan and Huang, 2002). Polyamine cationic lipids can also activate TLR2 and NLRP3 inflammasome pathways (Ito et al., 2009; Lonez et al., 2014). For example, Ma et al. reported that siRNA-cationic lipid complexes can induce strong type I and type II interferons, as well as activate signal transducer and activator of transcription 1 (STAT1) (Ma et al., 2005). DOTAP is a cationic lipid commonly used in research. DOTAP has dose-dependent toxicity (Dokka et al., 2000; Jensen et al., 2012); it was reported that increasing DOTAP content in lipid particles is associated with a corresponding increase in the toxicity and proinflammatory activity of the lipid particles in vitro and in vivo (Bian et al., 2012; Heidari et al., 2017; Lechanteur et al., 2018; Zhu et al., 2019). However, cationic lipids are often an indispensable component when formulating siRNA-SLNs; they are used to complex and lipophilize the hydrophilic siRNA by forming siRNA-cationic lipid complexes and thus increase the encapsulation of the negatively charged, hydrophilic siRNA in the SLNs (Granot and Peer, 2017; Hemati et al., 2019; Hwang et al., 2015; Inglut et al., 2020; Lv et al., 2006).

Previously, our group reported a TNF-α siRNA-encapsulated SLN formulation that showed strong activity against rheumatoid arthritis unresponsive to methotrexate (Aldayel et al., 2018). The siRNA-SLNs were prepared by encapsulating preformed siRNA and DOTAP complexes into SLNs prepared with lecithin, cholesterol, and an acid-sensitive stearoyl polyethylene glycol (PEG2000) conjugate (PHC). The present study was designed to study the effect of the amount of DOTAP used to complex siRNA on the cytotoxicity and proinflammatory activity of the resultant siRNA-SLNs. It was hypothesized that reducing the content of DOTAP, expressed as N/P ratio, in the siRNA-SLNs would reduce their cytotoxicity and proinflammatory activity. Unexpectedly, it was found that siRNA-SLNs prepared with the lowest N/P ratio were not necessarily the least cytotoxic or proinflammatory ones.

2. Materials and methods

2.1. Materials

DOTAP in chloroform and TopFluor® cholesterol were from Avanti Polar Lipids (Alabaster, AL). Control siRNA and TNF-α siRNA were from Integrated DNA Technology (IDT) (Coralville, IA). Lecithin was from Alfa Aesar (Ward Hill, MA). Cholesterol, lipopolysaccharide (LPS), and tetrahydrofuran (THF, HPLC grade) were from Sigma-Aldrich (St. Louis, MO). The PEG2000-hydrazone-stearic acid conjugate (PHC) was synthesized as previously described (Zhu et al., 2013a,b). FITC-labeled siRNA (BLOCK-iT™ Fluorescent Oligo) was from Invitrogen (Carlsbad, CA). ELISA kits (TNF-α and IL-6) were from BioLegend (San Diego, CA). Ultrafiltration devices (Amicon, 30 KDa molecular weight cutoff (MWCO)) were from Millipore Sigma (Burlington, MA). Dialysis devices (Float-A-Lyzer G2, 50 KDa MWCO) were from Spectrum Laboratories (Waltham, MA). All other solvents were of HPLC grade and were from Fisher Scientific (Waltham, MA). Mouse J774A.1 macrophages and mouse MPRO promyelocytic cell line were from the American Type Culture Collection (Manassas, VA). Dulbecco's Modified Eagle Medium (DMEM), Iscove's Modified Dulbecco's Medium (IMDM), fetal bovine serum, horse serum and penicillin/streptomycin (P/S), all from Gibco (Grand Island, NY).

2.2. Preparation of siRNA-SLNs

SLNs were prepared according to our previously published nanoprecipitation technique with slight modifications (Aldayel et al., 2018). To prepare one batch of SLNs, 680 μL of a DOTAP in chloroform solution (at different concentrations) was added dropwise into 500 μL of RNase-free water containing 15 μg siRNA under stirring at 900 rpm for 30 min. Methanol (1.3 mL) was added to form a clear monophase and stirred for 1 h. After that, 1 mL chloroform was added to facilitate phase separation. After the top aqueous layer was discarded, a chloroform solution containing 3.2 mg lecithin, 1.6 mg cholesterol, and 2 mg PHC were added to the bottom chloroform layer, and the whole mixture was then dried under nitrogen gas. The dried content was re-dissolved in 500 μL THF, which was then added dropwise into 5 mL RNase-free water and stirred at 900 rpm overnight to form nanoparticles. The resultant siRNA-SLNs were collected by ultra-centrifugation and then resuspended to the desired concentration in RNase-free water, 10 mM potassium phosphate buffer (PB, pH 7.4), 10 mM phosphate buffered saline (PBS, pH 7.4), or cell culture medium for further studies. TNF-α siRNA was used in the functional assay. Fluorescently labeled siRNA-SLNs were prepared either using FITC-labeled siRNA or by substituting 12.5% of the total cholesterol in the formulation with Top Fluor® cholesterol. Several formulations were prepared with different amount of DOTAP expressed in N/P ratio calculated as following:

$$\frac{N}{P} = \frac{\text{Number of moles of DOTAP}}{\text{Number of moles of siRNA} \times 50}$$

The 50 is based on the double stranded siRNA with 25 nucleotides in each strand.

2.3. In vitro characterization of siRNA-SLNs

The particle size, polydispersity index (PDI), and zeta potential of the siRNA-SLNs prepared at different N/P ratios were measured at 25 °C using a Malvern Zetasizer Nano ZS (Westborough, MA). The siRNA complexation efficiency with the DOTAP and the entrapment efficiency of the siRNA in the SLNs were determined using FITC-labeled siRNA following a previously reported method (Aldayel et al., 2018). The structure and morphology of the selected nanoparticles were determined using cryogenic electron microscopy (Cryo-EM). Briefly, concentrated siRNA-SLNs samples were placed in a lacey carbon film grid. The grids were then plunged frozen into liquid ethane. The frozen grids were imaged on a Thermo Fisher Scientific Glacios (Waltham, MA) operated at 200 kV and equipped with a Falcon 4 direct detector (Bouvette et al., 2022). Small angle and medium angle X-ray scattering (SAXS and MAXS, respectively) measurements were carried out using SAXSLabs Ganesha instrument with Cu K-alpha wavelength 1.5406 Å. The siRNA-SLNs was ultrafiltered, and the concentrated sample was loaded into a glass capillary with a diameter of 0.9 mm and a wall thickness of 0.01 mm. The filtrate was measured for background subtraction using the same SAXS settings. Scattering intensity was recorded from a q-range of 0.00497 to 0.4157 Åˆ-1. BioXTAS RAW 2.1.4 software and the GNOM package were used to carry out basic analyses such as the Guinier plot and the distance distribution p(r) function. The maximum linear dimension of the molecule, D_{max}, was calibrated for goodness-of-fit by enforcing a smooth zeroing of $P(D_{max})$. The release of the siRNA from nanoparticles was assessed by placing FITC-siRNA-SLNs equivalent to 12.5 μg FITC-siRNA in PB (10 mM, pH 7.4) inside a Float-A-Lyzer dialysis device (with 50 KDa MWCO), and the device was then submerged in 20 mL PB as the release medium. The release vessel was maintained in a MaxQ 5000 floor shaker incubator at 37 °C at 100 rpm. The fluorescence intensity of the released siRNA in the release medium was measured using a BioTek Synergy HT microplate reader (Winooski, VT). For modulated differential scanning calorimetry (mDSC), the SLNs were freeze-dried without any excipients using a VirTis Advantage Bench Top Tray Lyophilizer (Gardiner, NY) at shelf temperature − 40 °C under 80 mTorr. A QS20 DSC from TA Instruments (New Castle, DE) was used at a heating rate of 5 °C/min in the temperature range of −10 °C to 300 °C. An empty DSC aluminum pan was used as a reference. The mDSC experiment was repeated twice.

2.4. Cytotoxicity of siRNA-SLNs prepared at different N/P ratios

The cytotoxicity of siRNA-SLNs was determined using a standard MTT assay. J774A.1 macrophages were seeded in 96-well cell culture plates at a density of 20,000 cells/well in DMEM containing 10% FBS and 1% P/S. After overnight incubation, siRNA-SLNs were then added to the cells at various siRNA concentrations (i.e., 0.5, 2, 4, 6, 8, 10, and 12 μg/mL). After 24 h of incubation at 37 °C, 5% CO_2, cell viability was determined using an MTT reagent following the manufacturer's instruction. Cells without treatment were considered a control. When the MPRO cells were used, the cells were differentiated into the neutrophils by growing them in IMDM supplemented with 20% horse serum, 1% P/S, 10 μM all-trans retinoic acid, and 10 ng/mL granulocyte macrophage-colony stimulating factor (Lawson et al., 1998). The differentiated neutrophils were then seeded at a density of 5000 cells/well in complete medium. The siRNA-SLNs were incubated with the cells for 48 h with siRNA concentrations ranging from 2 to 24 μg/mL. Cell viability was calculated based on the percent relative absorbance at 550–595 nm of the treated versus the untreated cells.

2.5. Functionality assay of TNF-α siRNA-SLNs

To evaluate the function of the siRNA in the SLNs, TNF-α siRNA was used at selected N/P ratios. The TNF-α siRNA-encapsulated SLNs' ability to downregulate TNF-α release from macrophages in culture was evaluated. J774A.1 cell were seeded and incubated overnight in 96-well plates (10,000 cells/well) at 37 °C, 5% CO_2 in complete DMEM. After incubation, cells were treated with TNF-α siRNA-SLNs prepared at different N/P ratios, all containing 300 ng siRNA/well (3 μg/mL), dispersed in serum-free DMEM. Four hours later, an equivalent volume of DMEM containing 20% fetal bovine serum was added. After 44 additional hours of incubation, the culture medium was replaced with DMEM containing LPS (100 ng/mL). Cells that were left untreated with siRNA-SLNs but stimulated with LPS were considered a positive control, while cells that were untreated with the siRNA-SLNs and unstimulated with LPS were the negative control. Four hours later, cell culture medium was harvested, and TNF-α concentration in diluted samples was measured using a TNF-α ELISA kit. MTT assay was also performed to confirm cell viability.

2.6. In vitro IL-6 and TNF-α induction by SLNs, a measurement of proinflammatory activity

To evaluate the proinflammatory activity of siRNA-SLNs prepared at different N/P ratios, the ability of non-functional siRNA-SLNs to stimulate IL-6 and TNF-α production by J774A.1 macrophages and neutrophils differentiated from MPRO cells was determined. Cells were seeded in 96-well plates (20,000 cells/well) in supplemented DMEM or IMDM. After overnight incubation, the medium was removed (not removed in case of the MPRO cells) and siRNA-SLNs containing 2 μg siRNA were added in each well to reach a final concentration of 6 μg/mL. Cells that were untreated but stimulated with LPS were considered a positive control, while cells that were untreated and unstimulated were the negative control (Aldayel et al., 2018). After 8 h of incubation, cell culture medium was collected, and IL-6 and TNF-α content in the cell culture medium was quantified using ELISA kit. MTT assay was also used to confirm cell viability.

2.7. Release of DOTAP from selected SLNs as determined using an Azo dye method

The siRNA-SLNs prepared with N/P ratios of 1:1 and 12:1 but contained an equal amount of DOTAP were centrifuged and resuspended in 1 mL PB and placed in separate dialysis bags (8–10 KDa) of equal length. The bags were submerged in 3 mL of 1% Tween 20 in water as a release medium to maintain sink condition and agitated on a mini-orbital shaker at 300 rpm, 37 °C. At various time points, 400 μL of release medium was withdrawn and mixed with 100 μL of 0.5 mg/mL methyl orange (MO) and 680 μL chloroform. The mixture was stirred for one hour, and then 1.3 mL of methanol was added to form a single phase. Chloroform (1 mL) was then added to extract the MO-DOTAP complexes into the chloroform layer. The aqueous layer contained the unbound MO. The absorbance in chloroform phase was measured at 450 nm using a microplate reader. A calibration curve was constructed in the presence of other lipids in the SLNs to correlate DOTAP concentration and absorbance value (Cho et al., 1981; Cui and Mumper, 2002; Irfan et al., 2014; Nazar and Murtaza, 2014).

2.8. Statistical analysis

Statistical analysis was completed by performing one way ANOVA followed by Fisher's least significant difference procedure or student *t*-test. A $p \leq 0.05$ (two tail) was considered significant.

3. Results and discussion

3.1. Preparation and characterization of siRNA-SLNs

The cationic lipid is an essential component in siRNA-SLNs for the efficient entrapment or encapsulation of the siRNA into the SLNs; negatively charged siRNA and the positively charged cationic lipids form siRNA-cationic lipid complexes, which are then mixed with other lipid constituents to prepare SLNs. However, the cationic lipid is also in part responsible for the cytotoxicity and proinflammatory activity of the siRNA-SLNs (Abrams et al., 2010; Kim et al., 2007; Mendonça et al., 2020; Silva et al., 2019). To study the effect of the amount of DOTAP used to complex the siRNA on the cytotoxicity and proinflammatory activities of the resultant siRNA-SLNs, siRNA-SLNs were prepared at various N/P ratios (Table 1). The first step in preparing siRNA-SLNs was to condense the siRNA with different amounts of DOTAP to form siRNA-DOTAP complexes. The more DOTAP was added, the higher was the N/P ratio (Table 1). The siRNA-DOTAP complexes were formed in a water/methanol monophase and then partitioned into a chloroform phase, which was then mixed with other lipids including lecithin, cholesterol, and the acid-sensitive PHC. Upon evaporation of the chloroform, the mixture of the complexes and lipids was then dissolved in a THF

Table 1
Size, polydispersity index (PDI), and zeta potential of siRNA-SLNs and the complexation efficiency of siRNA to DOTAP at selected N/P ratios. Data are mean ± S.D. ($n \geq 3$). ND means not determined.

N/P ratio	DOTAP (mg)	siRNA complexation efficiency (%)	Particle size (nm)	PDI	Zeta potential (mV)
34:1	1.24	98.9 ± 0.7	141.4 ± 4.5	0.17 ± 0.02	5.8 ± 7.2
32:1	1.16	ND	141.3 ± 2.4	0.19 ± 0.02	-10.7 ± 6.6
28:1	1.02	93.1 ± 2.5	136.8 ± 6.2	0.21 ± 0.01	-17.4 ± 5.8
24:1	0.871	ND	130.9 ± 11.7	0.22 ± 0.03	-24.1 ± 5.8
20:1	0.727	88.0 ± 1.9	105.9 ± 6.2	0.22 ± 0.01	-34.4 ± 2.5
16:1	0.581	83.6 ± 1.4	102.3 ± 3.6	0.22 ± 0.03	-38.2 ± 2.4
12:1	0.436	80.7 ± 2.7	101.8 ± 10.1	0.23 ± 0.01	-40.7 ± 2.3
1:1	0.036	78.8 ± 2.8	81.3 ± 2.7	0.24 ± 0.004	-44.2 ± 3.1

solution, which was dropped into an aqueous phase under stirring to form siRNA-SLNs.

As shown in Table 1, siRNA-SLNs can be formed at all the N/P ratios tested. However, reducing the N/P ratio led to a gradual decrease in the size (i.e., from ~140 nm to 80 nm) as well as the zeta potential (i.e., ~ +6 mV to −44 mV) of the resultant siRNA-SLNs. All formulations had PDI values between 0.17 and 0.24 (Table 1), indicating narrow particle size distribution. The zeta potential reduction was expected as the reduction in N/P ratio was achieved by reducing the amount of the cationic DOTAP lipid used to complex a fixed amount of siRNA. The reduction in the particle size when the N/P ratio was reduced was likely due to the composition change in the resultant siRNA-SLNs (Carbone et al., 2012). Reducing the N/P ratio led to a decrease in the complexation efficacy of siRNA (Table 1). For example, almost 100% of the siRNA was complexed with the DOTAP at the N/P ratios 34:1, but at the N/P ratios of 12:1 and 1:1, only about 80% of the siRNA was complexed (Table 1). Therefore, due to the method by which the siRNA-SLNs were prepared, the amount of siRNA in siRNA-SLNs prepared with different N/P ratio was likely different. However, the encapsulation efficiency of the siRNA in the final siRNA-SLNs was close to 100% in all the siRNA-SLNs prepared. The in vitro release study data demonstrated that all the siRNA-SLNs showed a minimal burst followed by a slower release of siRNA, with around 5–12% of siRNA released over 7 days (Fig. 1). The lack of a significant burst release of siRNA from the SLNs prepared at different N/P ratios were likely due to the removal of the un-complexed siRNA in the aqueous phase during the preparation step. Moreover, the complexation and condensation of siRNA with DOTAP should have enabled the encapsulation of the siRNA inside the SLNs. Overall, the N/P ratio affected the rate by which the siRNA was released from the various siRNA-SLNs (Fig. 1); the siRNA release was fastest from the siRNA-SLNs prepared at the N/P ratio of 1:1 followed by siRNA-SLNs prepared at the N/P ratios of 34:1 and 12:1 (Fig. 1), and surprisingly slowest from the siRNA-SLNs prepared at the N/P ratio of 20:1 (Fig. 1), likely due to its unique composition. Shown in Fig. 2 are representative Cryo-EM micrographs of the siRNA-SLNs prepared at the N/P ratio of 34:1, 12:1, or 1:1. The siRNA-SLNs prepared at the N/P ratio of 1:1 are spherical (about 50 nm or smaller), with an unilamellar double-layer shell (Fig. 2A). The siRNA-SLNs prepared at the N/P ratio 34:1 showed large (about 80 nm), more complex structure and morphology, with many showing multilamellar layers (Fig. 2C). The siRNA-SLNs prepared at the N/P ratio of 12:1 were unique with a mixture of unilamellar spheres and some particles with blebs (Fig. 2B) around 70 nm. Clearly, the N/P ratio used to prepare the siRNA-SLNs significantly affected the morphologies

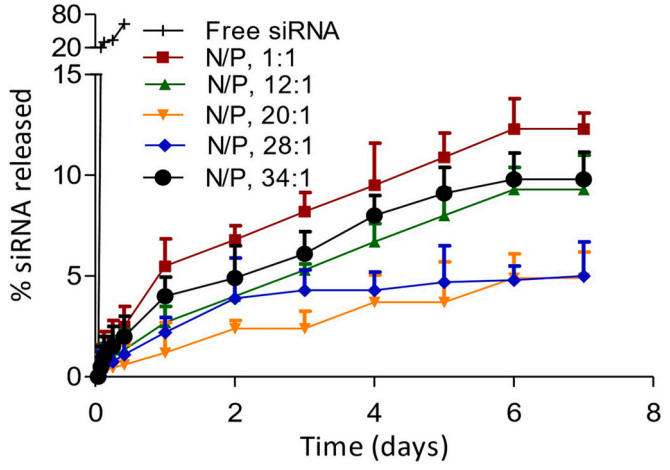

Fig. 1. In vitro release profiles of siRNA from SLNs prepared at N/P ratios 34:1, 28:1, 20:1, 12:1, and 1:1 in 10 mM PB (pH 7.4). As a control, the diffusion of free siRNA across the dialysis membrane was also monitored. Data are mean ± S.D. ($n = 3$).

and structures of the resultant siRNA-SLNs. The size and lamellarity structural differences between the siRNA-SLNs prepared at the N/P ratio of 34:1, 12:1, or 1:1 shown in the Cryo-EM micrographs were in alignment with data from SAXS and MAXS (Fig. 3). The broad peak around the q value of 0.1 (A^{-1}) of the MAXS profiles in siRNA-SLNs prepared at the N/P ratios 12:1 or 1:1 typically signifies a unilamellar architecture, as multilamellar concentric spheres tend to produce a narrower and sharper peak (Fig. 3A). Indeed, the comparatively narrow peak around the q value of 0.1 (A^{-1}) observed in the MAXS profile of the siRNA-SLN at the N/P ratio of 34:1 suggested a population of siRNA-SLNs exhibiting a multilamellar structure, which is supported by the Cryo-EM micrographs (Fig. 2C). While the MAXS profiles reveal insights into the internal structure of the siRNA-SLNs, the SAXS profile region provides information about the overall size and shape (Fig. 3B). Through pair distribution function analysis of the SAXS curve in Fig. 3B, it was determined that the maximum distance between pairs of electrons in the siRNA-SLNs (D_{max}) values to be 477, 635, and 697 Å for siRNA-SLNs prepared at the N/P ratios of 1:1, 12:1, or 34:1, respectively. These measurements align closely with the diameter estimations of the siRNA-SLNs derived from the cryo-EM micrographs. Furthermore, the relative particle sizes were consistent with the dynamic light scattering data (Table 1), wherein the hydrodynamic diameters of the siRNA-SLNs prepared at the N/P ratios of 1:1, 12:1, and 34:1 were found to be 813, 1018, and 1414 Å, respectively.

3.2. *In vitro cytotoxicity of siRNA-SLNs prepared at different N/P ratios*

The siRNA-SLNs prepared at the N/P ratio of 34:1 showed the highest cytotoxicity to the J774A.1 macrophages in a dose-dependent manner with a half maximal inhibitory concentration (IC_{50}) of 8.1 ± 0.37 μg/mL (Fig. 4A-B). Reducing the N/P ratio to 20:1, 16:1, and 12:1 led to a reduction in the cytotoxicity in the macrophages, with IC_{50} values larger than that at the N/P ratio of 34:1. The IC_{50} values of siRNA-SLNs prepared at the N/P ratios of 20:1, 16:1 and 12:1 were 23.9 ± 5.73, 26.5 ± 5.92, and 26.1 ± 3.97 μg/mL, respectively (Fig. 4B). DOTAP is known to interact with, and destabilize, cell membrane and inhibit the activity of Na/K pumps (Soenen et al., 2009; Wei et al., 2015). Therefore, it was expected that siRNA-SLNs prepared at a lower N/P ratio would be less cytotoxic than the ones prepared with relative higher N/P ratios. Surprisingly, the siRNA-SLNs prepared at N/P ratios lower than 12:1 were increasingly more cytotoxic than the ones prepared at the N/P ratio of 12:1. For example, the IC_{50} values of the siRNA-SLNs prepared at the N/P ratios of 8:1, 4:1, and 1:1 were 22.1 ± 4.06, 18.9 ± 0.94, and 17.4 ± 2.25 μg/mL, respectively (Fig. 4B). Overall, it appears that the siRNA-SLNs prepared at the N/P ratios of 16:1 and 12:1 showed the least cytotoxicity, not the ones that were prepared at the N/P ratio of 1:1 (i.e., with the least amount of DOTAP) (Fig. 4B). The same trend was also observed with the neutrophils differentiated from the MPRO cells (Fig. 4C-D); the cytotoxic activity of the siRNA-SLNs prepared at the N/P ratio of 12:1 was lower than that of the siRNA-SLNs prepared at the N/P ratio of 34:1 or 1:1. In the present study, macrophage and neutrophil cell lines were used to study the cytotoxicity of the siRNA-SLNs, because both neutrophils and macrophages play key roles in inflammatory responses (Bian et al., 2012; Zhang and Wang, 2014).

3.3. *In vitro functionality of TNF-α siRNA in siRNA-SLNs prepared at different N/P ratios*

To test the function of the siRNA in the SLNs, the ability of the siRNA-SLNs prepared at various N/P ratios in inhibiting TNF-α production by macrophages stimulated with LPS in culture was evaluated. As shown in Fig. 5, all the TNF-α siRNA-SLNs tested significantly inhibited TNF-α cytokine production by the J774A.1 macrophages. The TNF-α siRNA in SLNs prepared at N/P ratios 34:1, 12:1, and 1:1 were equally effective in down-regulating TNF-α expression, but the TNF-α siRNA-SLNs prepared at the N/P ratio of 20:1 and 28:1 seemed to be the least effective. It is not

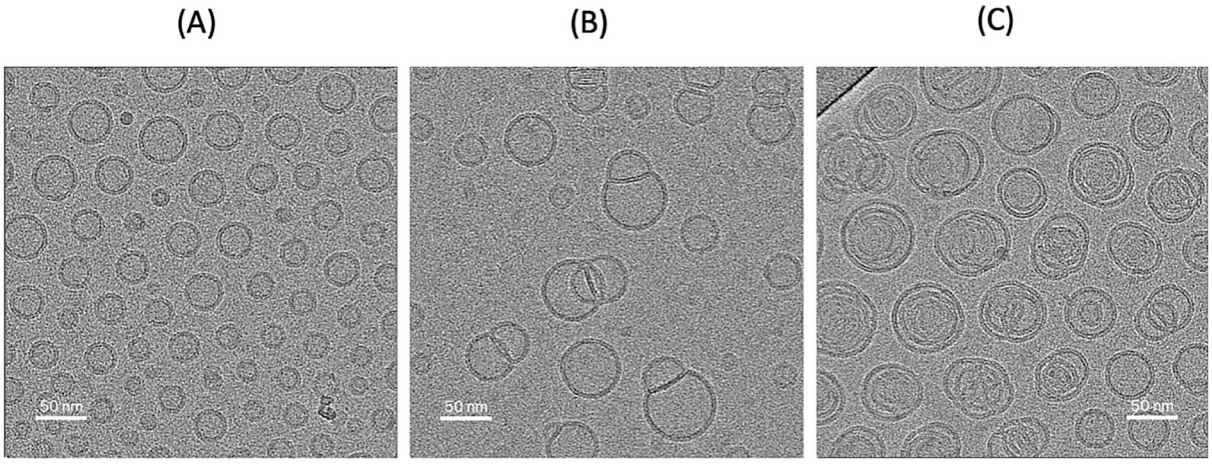

Fig. 2. Representative Cryo-EM micrographs of siRNA-SLNs prepared at a N/P ratio of (A) 1:1, (B) 12:1, or (C) 34:1.

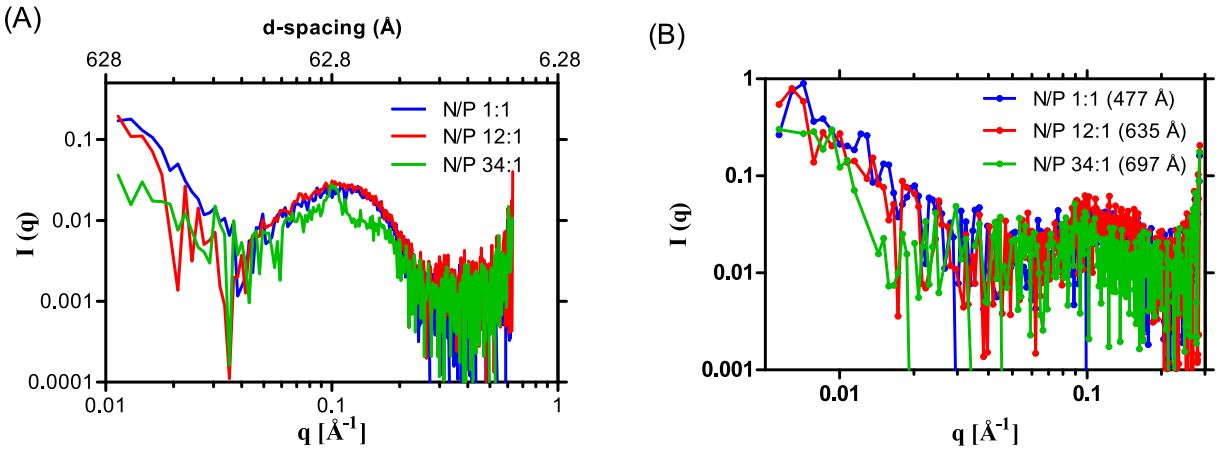

Fig. 3. (A) Medium and (B) small angle X-ray scattering profiles of siRNA-SLNs prepared at N/P ratio of 34:1, 12:1, or 1:1 with peak at d-spacing around 62.8 Å (n = 2); with the corresponding maximum distance between pair of electrons (D_{max}) values in the parentheses (447, 635, and 697 Å, respectively). The D_{max} values were calculated from the SAXS scattering profiles using GNOM package.

known whether the siRNA-SLNs prepared at the N/P ratio of 20:1 and 28:1 had a reduced cell uptake, or the TNF-α siRNA in those siRNA-SLNs had a reduced access to TNF-α mRNA in cells upon transfection. In fact, the in vitro siRNA release data in Fig. 1 showed that the release of siRNA from the siRNA-SLNs prepared at the N/P ratios of 20:1 and 28:1 were the slowest and the second slowest, respectively, among the various siRNA-SLNs tested. The siRNA-SLNs prepared at N/P ratios of 12:1 and 1:1 were chosen for additional studies, due to their similarity in particle size, zeta potential, siRNA complexation efficacy, ability to down-regulate TNF-α expression by J774A.1 cells in culture, and to a certain extent morphology and structure.

3.4. TNF-α and IL-6 production in vitro upon stimulation with siRNA-SLNs

Cytokines play an important role in orchestrating and controlling the inflammatory process, and excessive cytokine production can result in serious adverse reactions. TNF-α is a potent multifunctional cytokine, exerting regulatory, inflammatory, and cytotoxic effects in a wide range of cells (Feuerstein et al., 1994). IL-6 is a soluble mediator and is typically described as a common proinflammatory cytokine responsible for immune response activation (Kany et al., 2019). After the immune system recognizes cationic lipids such as DOTAP, immune cells secrete IL-6 that leads to an increase in vascular permeability and swelling associated with inflammation, and thus this proinflammatory cytokine can be used as a biomarker of immunotoxicity (Elsabahy and Wooley, 2013). Cationic lipids such as DOTAP can help induce desired cytokine production when used in vaccine formulations (Mansury et al., 2019; Tada et al., 2015). However, the presence of DOTAP in siRNA-SLNs, especially when excessive, can be detrimental due to its undesirable immunotoxicity. As shown in Fig. 6, in both J774A.1 macrophages and in neutrophils differentiated from MPRO cells, siRNA-SLNs prepared at the N/P ratio of 34:1 induced higher TNF-α and IL-6 release than those prepared at the lower N/P ratios of 12:1 and 1:1, and the siRNA-SLNs prepared at the N/P ratio of 12:1 induced similar levels of the TNF-α and IL-6 cytokines as the siRNA-SLNs prepared at the N/P ratio of 1:1 (even lower level of TNF-α in the J774A.1 cells) (Fig. 6). The size of nanoparticles could contribute to their immunogenicity. For example, it was reported that large polypyrrole nanoparticles induced a stronger innate immunity than smaller nanoparticles (Kim et al., 2011). Therefore, the relatively larger size of the siRNA-SLNs prepared at the N/P ratio of 34:1 may also have contributed to a certain extent to their higher TNF-α and IL-6 inducing activity than the relatively smaller siRNA-SLNs prepared at N/P ratios of 12:1 or 1:1. Additionally, the positive zeta potential value of the siRNA-SLNs prepared at the N/P ratio of 34:1, as compared to the negative zeta potential values of the siRNA-SLNs prepared at the N/P ratio of 12:1 or 1:1, likely have also contributed to the higher proinflammatory cytokine production (Kedmi et al., 2010).

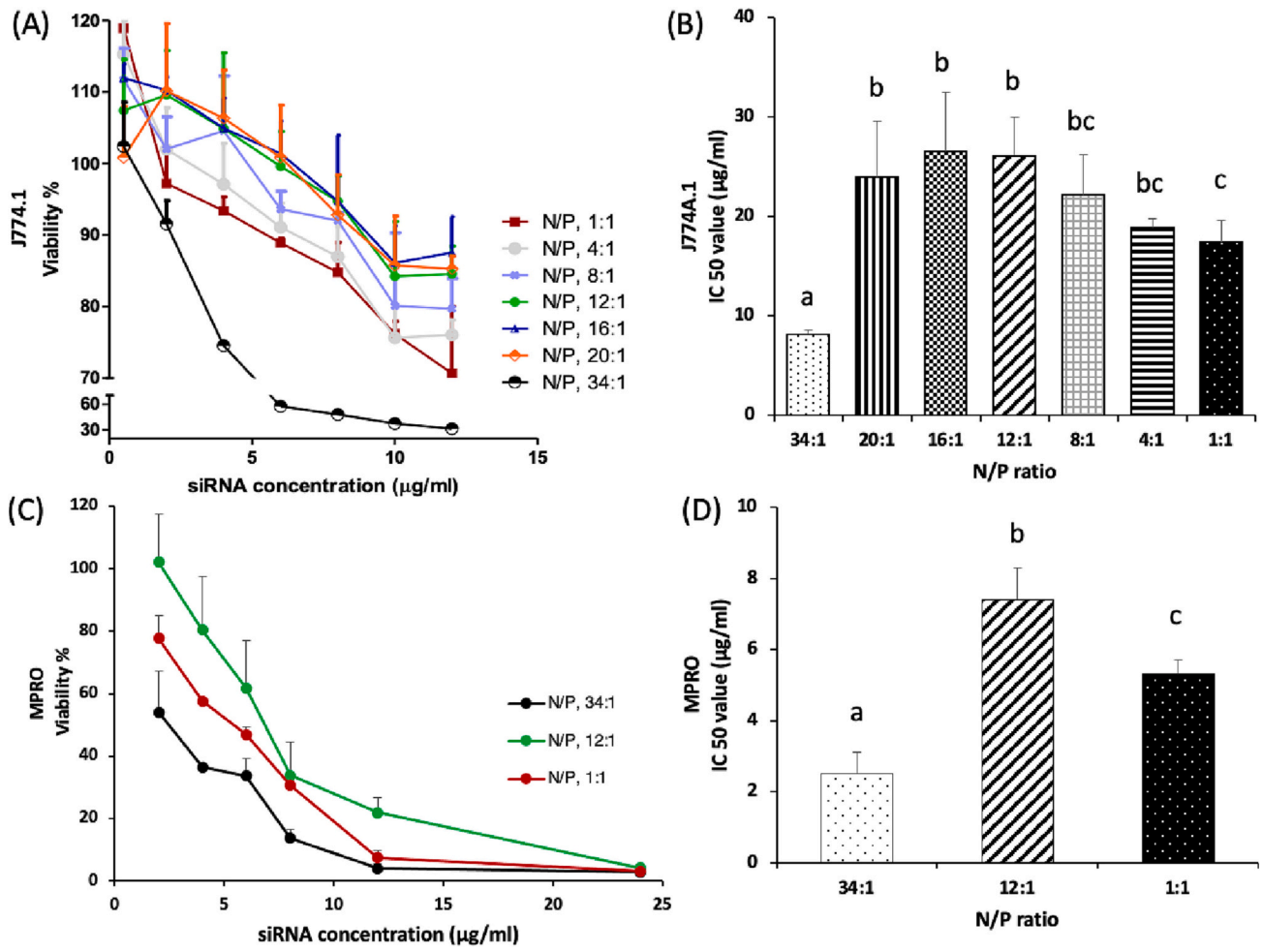

Fig. 4. The cytotoxicity of siRNA-SLNs prepared at different N/P ratios in J774A.1 macrophage cells (A-B) and in neutrophils differentiated from MPRO promyelocytic cells (C—D). Data are mean ± S.D. (n = 3). The experiment was also repeated in the J774A.1 cells independently with siRNA-SLNs prepared with selected N/P ratios, and a similar result was obtained. ($^{a\text{-}c}$, $p < 0.05$).

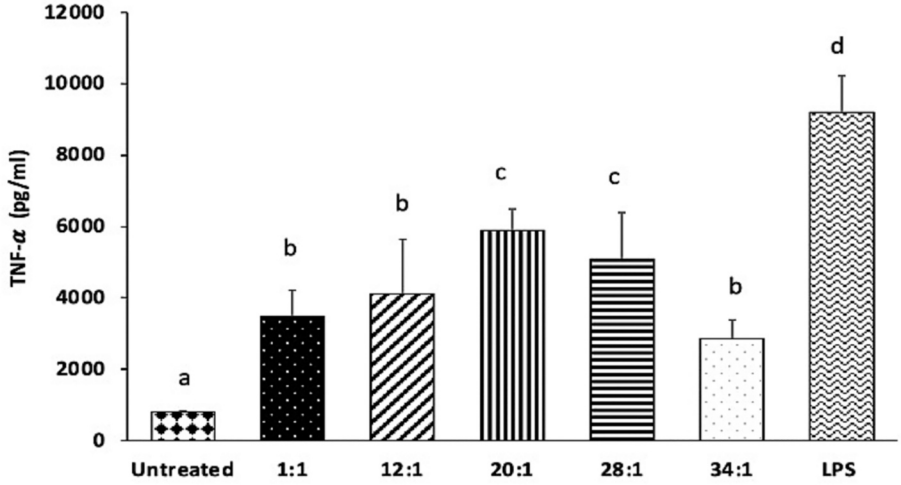

Fig. 5. TNF-α siRNA's activity in downregulating TNF-α cytokine production in macrophages in culture. The TNF-α siRNA-SLNs prepared at different N/P ratios (34:1, 28:1, 20:1, 12:1, and 1:1) were incubated with J774A.1 cells for 48 h, followed by four additional hours of incubation with 100 ng/mL LPS. Data are mean ± S.D. ($n = 4$). ($^{a\text{-}d}$, $p < 0.05$).

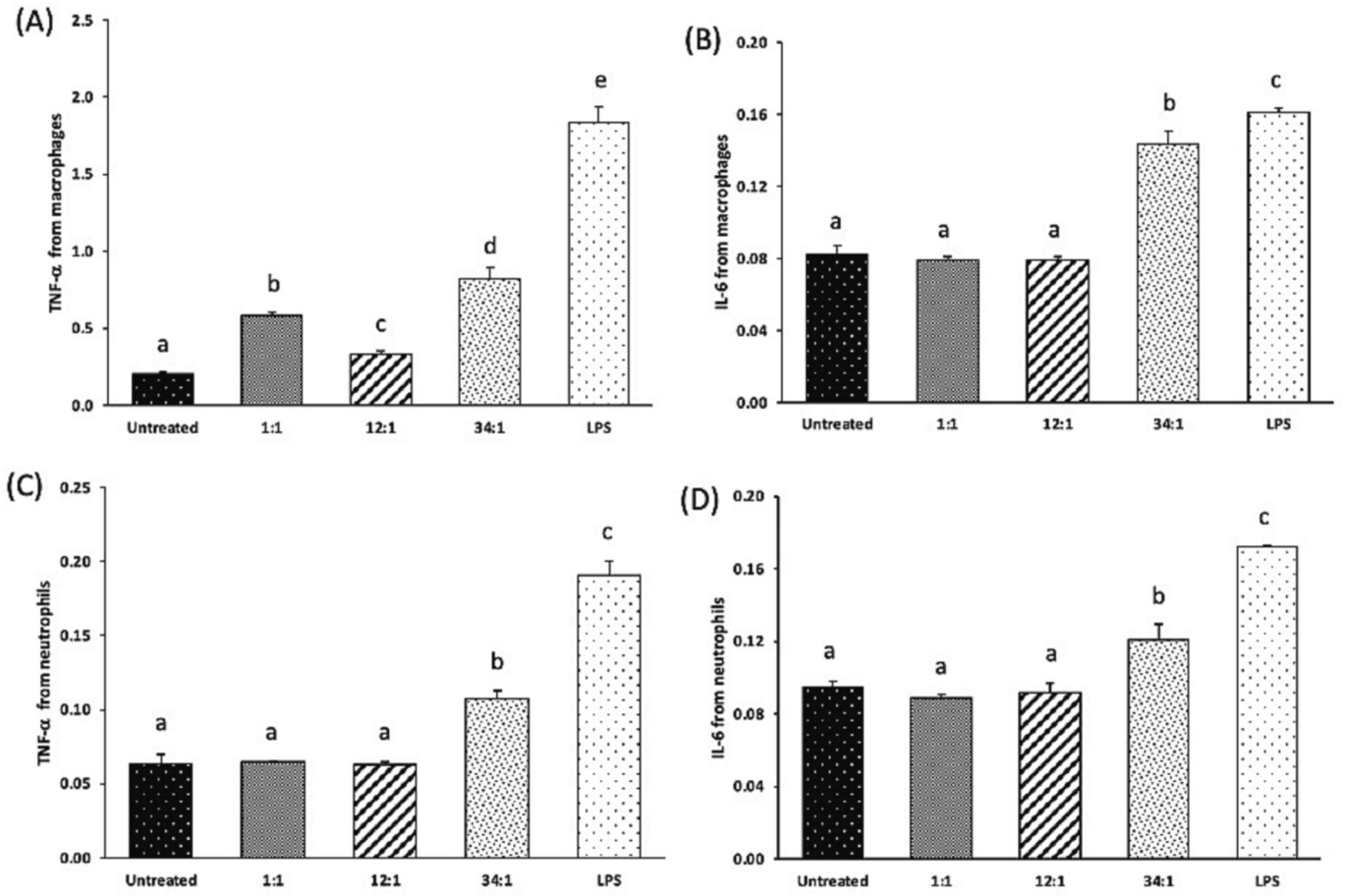

Fig. 6. TNF-α (A & C) and IL-6 (B & D) production by J774A.1 macrophages (A-B) and neutrophils differentiated from MPRO cells (C—D) after 8 h of incubation with siRNA-SLNs prepared at N/P ratios of 34:1, 12:1, or 1:1. Data are mean ± S.D. (n = 3) ($^{a\text{-}e}$, $p < 0.05$). Y axis represents OD value at 450 nm in ELISA.

However, the key reason behind the stronger proinflammatory activity of the siRNA-SLNs prepared at a N/P ratio of 34:1 was likely the excess amount of DOTAP in the siRNA-SLNs.

3.5. *In vitro DOTAP release from siRNA-SLNs prepared at N/P ratios of 12:1 or 1:1*

TNF-α siRNA-SLNs prepared at the N/P ratios of 12:1 or 1:1 were similarly effective in inhibiting TNF-α production (Fig. 5), and siRNA-SLNs prepared with control siRNA at the N/P ratios of 12:1 or 1:1 showed similarly low proinflammatory activity (Fig. 6). However, the cytotoxicity data in Fig. 4 showed that the siRNA-SLNs prepared at the N/P ratio of 12:1 were less cytotoxic than the ones prepared at the N/P ratio of 1:1, which was unexpected; instead it was expected that the siRNA-SLNs prepared at the N/P ratio of 1:1 would be less cytotoxic because they contained less DOTAP. A comparison of the mDSC graphs of the siRNA-SLNs prepared at N/P ratios of 34:1, 12:1 and 1:1 failed to reveal any significant difference (Fig. 7). Since DOTAP is the most

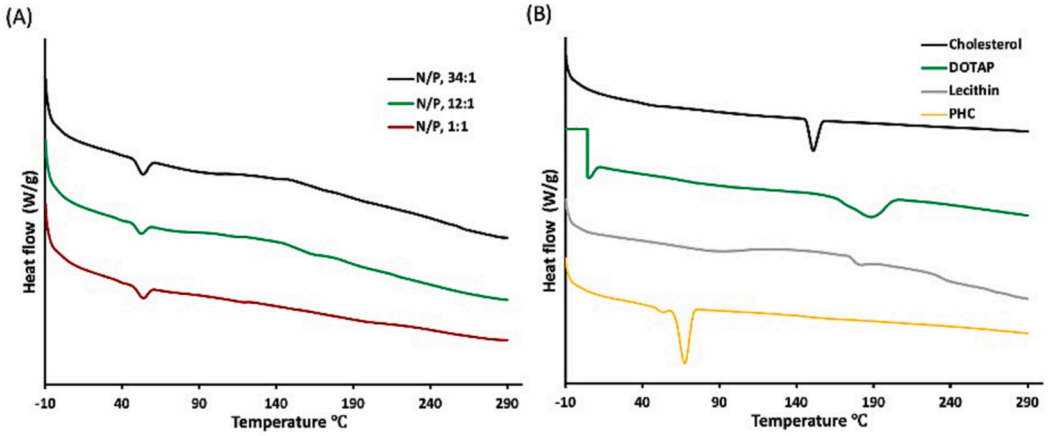

Fig. 7. (A) mDSC thermograms of siRNA-SLNs prepared at N/P ratios of 34:1, 12:1 or 1:1. Shown in B are the mDSC thermograms of pure cholesterol, DOTAP, lecithin, and PHC as controls. Experiment was repeated twice with similar results.

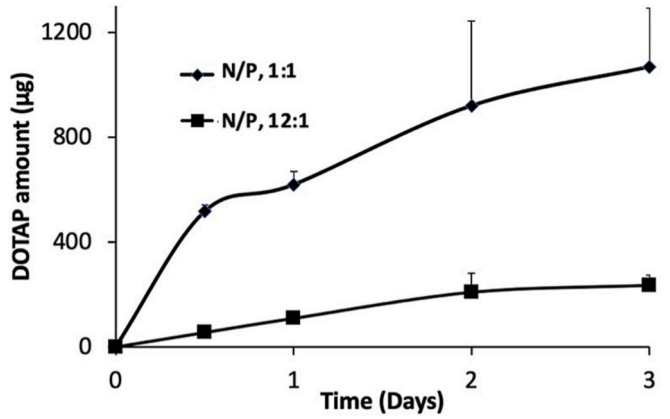

Fig. 8. In vitro release of DOTAP from siRNA-SLNs prepared at N/P ratios of 1:1 or 12:1 in 1% Tween 20 solution.

cytotoxic component in the siRNA-SLNs, we therefore tested the release of DOTAP from siRNA-SLNs prepared at N/P ratios of 12:1 and 1:1. DOTAP in the release medium (i.e., a 1% Tween 20 solution) was measured after it was complexed with MO, an Azo dye, which was previously used to quantify quaternary ammonium compounds (Cho et al., 1981; Irfan et al., 2014). MO is a negatively charged hydrophilic Azo dye, which can electrostatically bind to the cationic DOTAP to form lipophilic MO-DOTAP complexes. The complexes were then extracted from the release medium to a chloroform phase and quantified using UV–Vis spectrometry. Fig. 8 showed that the release of DOTAP from the siRNA-SLNs prepared at the N/P ratio of 1:1 was faster than that from the siRNA-SLNs prepared at the N/P ratio of 12:1, which may explain the relatively higher cytotoxicity of the siRNA-SLNs prepared at the N/P ratio of 1:1. It was possible that at the N/P ratio of 12:1, DOTAP and siRNA complexed more efficiently, forming more condensed and hydrophobic DOTAP-siRNA complexes, allowing better incorporation of the complexes in the core of the resultant SLNs. In contrast, at the N/P ratio of 1:1, the DOTAP-siRNA complexes formed were not as condensed, and thus were not well incorporated in the core of the SLNs. Also, the slower release of siRNA from SLNs (N/P, 12:1) compared to from 1:1, as shown in Fig. 1, supports the hypothesis of more efficient condensation of siRNA/DOTAP in the siRNA-SLNs prepared at the N/P ratio of 12:1. In other words, the unique composition and structure of the siRNA-SLNs prepared at the N/P ratios of 12:1 rendered them the desirable properties concerning cytotoxicity, proinflammatory activity, as well as functionality.

We have evaluated the blood as well as organ pharmacokinetics of the siRNA-SLNs prepared at the N/P ratio of 12:1 in a mouse model (Fig. S1), which showed an elimination phase half-life of ~70 h in blood (Table S1). We have also compared the biodistribution of the siRNA-SLNs prepared at the N/P ratios of 12:1 vs. 34:1 and demonstrated that the N/P ratio significantly affected the distribution patterns (Fig. S2). Therefore, the siRNA-SLNs prepared at the N/P ratio of 12:1 may show different pharmacodynamic and toxicity profiles as compared to the siRNA-SLNs prepared at the N/P ratio of 34:1. However, it is noted that the siRNA-SLNs prepared at the N/P ratio of 12:1 may not be the least toxic and proinflammatory ones if tested in vivo. Nonetheless, our findings demonstrated that changing the ratio of the cationic lipid and siRNA in SLNs not only altered the structure and morphology of the resultant siRNA-SLNs, but also resulted in siRNA-SLNs with reduced cytotoxicity and proinflammatory activity, without sacrificing the function of the siRNA-SLNs.

In general, the structural features of the cationic lipids in SLNs greatly affect the cytotoxicity of the SLNs. Pinnaduwage et al. showed that the one-tailed cationic lipid cetyl trimethylammonium bromide (CTAB) was more cytotoxic than the two-tailed DOTMA (Pinnaduwage et al., 1989). However, Tang and Hughes demonstrated that the one tail 6-lauroxyhexyl ornithinate (LHON) was of lower cytotoxicity compared with the two-tailed DOTAP (Tang and Hughes, 1999). On the other hand, the cytotoxicity of cationic lipids is lowered when the linker bond is degradable. Most of the linker bonds are either ether, ester, amide, or carbamate. The stable ether linker makes cationic lipids less biodegradable and hence more cytotoxic. Cationic lipids with ester bonds such as DOTAP in the linker zone are more biodegradable and associated with less cytotoxicity in cell culture (Freedland et al., 1996; Joon Sig Choi et al., 2001). The cytotoxicity of cationic lipids is also strongly connected to the cationic nature of the lipid head groups. Quaternary amine amphiphiles such as DOTMA and DOTAP are generally more cytotoxic than their tertiary amine counterparts (Bottega and Epand, 1992; Cui et al., 2018). Recently, ionizable lipids are used as a safer alternative to permanently charged cationic lipids to reduce the toxicity and immunogenicity of lipid nanoparticless. Ionizable lipids are positively charged in low pH conditions and can condense siRNA during the preparation step but become neutral at physiologic pH and thus minimizing their cytotoxicity (Han et al., 2021). The 1,2-dilinoleyloxy-*N*,*N*-dimethyl-3-aminopropane (DLin-DMA) is an example of ionizable lipid. DLin-DMA was further modified to (6Z,9Z,28Z,31Z)-heptatriaconta-6,9,28,31tetraen-19-yl 4-(dimethylamino) butanoate (DLin-MC3-DMA) and used to formulate the FDA approved siRNA product Onpattro® (Ickenstein and Garidel, 2019). A future direction of replacing the DOTAP in the siRNA-SLNs with an ionizable lipid such as the DLin-MC3-DMA may make the siRNA-SLNs even less cytotoxic and proinflammatory.

4. Conclusions

In our efforts to study the effect of the amount of cationic lipid used to complex the siRNA on the cytotoxicity and proinflammatory activities of the resultant siRNA-SLNs, a DOTAP to siRNA N/P ratio that rendered the resultant siRNA-SLNs with the least cytotoxicity and proinflammatory activity was identified. Surprisingly, the siRNA-SLNs prepared with the lowest amount of the cationic lipid (i.e., the lowest N/P ratio) were not the least cytotoxic and proinflammatory, likely because the N/P ratio significantly affected the morphology, structural, and physical properties of the resultant siRNA-SLNs (e.g., size, zeta potential, siRNA content, and release profile).

Declaration of Competing Interest

Z Cui reports a relationship with Via Therapeutics. A financial conflict of interest management plan is available at UT Austin.

Data availability

Data will be made available on request.

Acknowledgments

This work was supported in part by Via Therapeutics, LLC (NIH R43AR074360 to JJK and ZC) and the Mannino Fellowship in Pharmacy at UT Austin (to ZC). MSH was supported in part by an Egyptian Government Scholarship. We would like to acknowledge Axel Brilot and Evan Schwartz in the Electron Microscopy Facility at UT Austin for their support and help.

Appendix A. Supplementary data

Supplementary data to this article can be found online at https://doi.org/10.1016/j.ijpx.2023.100197.

References

Abrams, M.T., Koser, M.L., Seitzer, J., Williams, S.C., Dipietro, M.A., Wang, W., Shaw, A. W., Mao, X., Jadhav, V., Davide, J.P., Burke, P.A., Sachs, A.B., Stirdivant, S.M., Sepp-

Lorenzino, L., 2010. Evaluation of efficacy, biodistribution, and inflammation for a potent siRNA nanoparticle: effect of dexamethasone co-treatment. Mol. Ther. 18 (1), 171–180. https://doi.org/10.1038/mt.2009.208.

Aldayel, A.M., O'Mary, H.L., Valdes, S.A., Li, X., Thakkar, S.G., Mustafa, B.E., Cui, Z., 2018. Lipid nanoparticles with minimum burst release of TNF-α siRNA show strong activity against rheumatoid arthritis unresponsive to methotrexate. J. Control. Release 283, 280–289. https://doi.org/10.1016/j.jconrel.2018.05.035.

Bian, Z., Guo, Y., Ha, B., Zen, K., Liu, Y., 2012. Regulation of the Inflammatory Response: Enhancing Neutrophil Infiltration under Chronic Inflammatory Conditions. J. Immunol. 188, 844–853. https://doi.org/10.4049/jimmunol.1101736.

Bottega, R., Epand, R.M., 1992. Inhibition of Protein Kinase C by Cationic Amphiphiles. Biochemistry. 31 (37), 9025–9030. https://doi.org/10.1021/bi00152a045.

Bouvette, J., Huang, Q., Riccio, A.A., Copeland, W.C., Bartesaghi, A., Borgnia, M.J., 2022. Automated systematic evaluation of cryo-EM specimens with SmartScope. Elife 11, e80047. https://doi.org/10.7554/ELIFE.80047.

Carbone, C., Tomasello, B., Ruozi, B., Renis, M., Puglisi, G., 2012. Preparation and optimization of PIT solid lipid nanoparticles via statistical factorial design. Eur. J. Med. Chem. 49, 110–117. https://doi.org/10.1016/j.ejmech.2012.01.001.

Cho, Y.M., Lee, W.K., Kim, B.K., 1981. Studies on the interaction of azo dyes with cationic surfactant (I). Arch. Pharm. Res. 4, 75–84. https://doi.org/10.1007/BF02855749.

Choi, Joon Sig, Lee, Eun Jung, Jang, Hyung Suk, Park, Jong Sang, 2001. New cationic liposomes for gene transfer into mammalian cells with high efficiency and low toxicity. Bioconjug. Chem. 12 (1), 108–113. https://doi.org/10.1021/bc000081o.

Cui, Z., Mumper, R.J., 2002. Coating of cationized protein on engineered nanoparticles results in enhanced immune responses. Int. J. Pharm. 238 (1–2), 229–239. https://doi.org/10.1016/S0378-5173(02)00079-0.

Cui, S., Wang, Y., Gong, Y., Lin, X., Zhao, Y., Zhi, D., Zhou, Q., Zhang, S., 2018. Correlation of the cytotoxic effects of cationic lipids with their headgroups. Toxicol. Res. (Camb). 7 (3), 473–479. https://doi.org/10.1039/c8tx00005k.

Curreri, A., Sankholkar, D., Mitragotri, S., Zhao, Z., 2022. RNA Therapeutics in the Clinic. Bioeng. Transl. Med. 8 (1), e10374 https://doi.org/10.1002/btm2.10374.

Dokka, S., Toledo, D., Shi, X., Castranova, V., Rojanasakul, Y., 2000. Oxygen radical-mediated pulmonary toxicity induced by some cationic liposomes. Pharm. Res. 17, 521–525. https://doi.org/10.1023/A:1007504613351.

Elsabahy, M., Wooley, K.L., 2013. Cytokines as biomarkers of nanoparticle immunotoxicity. Chem. Soc. Rev. 42 (12), 5552–5576. https://doi.org/10.1039/c3cs60064e.

Feuerstein, G.Z., Liu, T., Barone, F.C., 1994. Cytokines, inflammation, and brain injury: Role of tumor necrosis factor-alpha. Cerebrovasc.Brain Metab.Rev. 6 (4), 341–360.

Freedland, S.J., Malone, R.W., Borchers, H.M., Zadourian, Z., Malone, J.G., Bennett, M. J., Nantz, M.H., Li, J.H., Gumerlock, P.H., Erickson, K.L., 1996. Toxicity of cationic lipid-ribozyme complexes in human prostate tumor cells can mimic ribozyme activity. Biochem. Mol. Med. 59 (2), 144–153. https://doi.org/10.1006/bmme.1996.0080.

Granot, Y., Peer, D., 2017. Delivering the right message: challenges and opportunities in lipid nanoparticles-mediated modified mRNA therapeutics—an innate immune system standpoint. Semin. Immunol. 34, 68–77. Academic Press. https://doi.org/10.1016/j.smim.2017.08.015. Academic Press.

Han, X., Zhang, H., Butowska, K., Swingle, K.L., Alameh, M.G., Weissman, D., Mitchell, M.J., 2021. An ionizable lipid toolbox for RNA delivery. Nat. Commun. 12 (1), 7233. https://doi.org/10.1038/s41467-021-27493-0.

Hanafy, M.S., Hufnagel, S., Trementozzi, A.N., Sakran, W., Stachowiak, J.C., Koleng, J.J., Cui, Z., 2021. PD-1 siRNA-encapsulated solid lipid nanoparticles downregulate PD-1 expression by macrophages and inhibit tumor growth: PD-1 siRNA-encapsulated solid lipid nanoparticles. AAPS PharmSciTech 22, 1–8. https://doi.org/10.1208/s12249-021-01933-y.

Heidari, Z., Arora, J.S., Datta, D., John, V.T., Kumar, N., Bansal, G.P., 2017. Impact of the charge Ratio on the in Vivo Immunogenicity of Lipoplexes. Pharm. Res. 34, 1796–1804. https://doi.org/10.1007/s11095-017-2187-2.

Hemati, M., Haghiralsadat, F., Yazdian, F., Jafari, F., Moradi, A., Malekpour-Dehkordi, Z., 2019. Development and characterization of a novel cationic PEGylated niosome-encapsulated forms of doxorubicin, quercetin and siRNA for the treatment of cancer by using combination therapy. Artif. Cells Nanomed. Biotechnol. 47 (1), 1295–1311. https://doi.org/10.1080/21691401.2018.1489271.

Hwang, T.L., Aljuffali, I.A., Lin, C.F., Chang, Y.T., Fang, J.Y., 2015. Cationic additives in nanosystems activate cytotoxicity and inflammatory response of human neutrophils: Lipid nanoparticles versus polymeric nanoparticles. Int. J. Nanomedicine 10, 371. https://doi.org/10.2147/IJN.S73017.

Ickenstein, L.M., Garidel, P., 2019. Lipid-based nanoparticle formulations for small molecules and RNA drugs. Expert Opin. Drug Deliv. 16 (11), 1205–1226. https://doi.org/10.1080/17425247.2019.1669558.

Inglut, C.T., Sorrin, A.J., Kuruppu, T., Vig, S., Cicalo, J., Ahmad, H., Huang, H.C., 2020. Immunological and toxicological considerations for the design of liposomes. Nanomaterials. 10 (2), 190. https://doi.org/10.3390/nano10020190.

Irfan, M., Usman, M., Mansha, A., Rasool, N., Ibrahim, M., Rana, U.A., Siddiq, M., Zia-Ul-Haq, M., Jaafar, H.Z.E., Khan, S.U.D., 2014. Thermodynamic and spectroscopic investigation of interactions between reactive red 223 and reactive orange 122 anionic dyes and cetyltrimethyl ammonium bromide (CTAB) cationic surfactant in aqueous solution. Sci. World J. 2014 https://doi.org/10.1155/2014/540975.

Ito, Y., Kawakami, S., Charoensit, P., Higuchi, Y., Hashida, M., 2009. Evaluation of proinflammatory cytokine production and liver injury induced by plasmid DNA/cationic liposome complexes with various mixing ratios in mice. Eur. J. Pharm. Biopharm. 71 (2), 303–309. https://doi.org/10.1016/j.ejpb.2008.09.005.

Jensen, D.K., Jensen, L.B., Koocheki, S., Bengtson, L., Cun, D., Nielsen, H.M., Foged, C., 2012. Design of an inhalable dry powder formulation of DOTAP-modified PLGA nanoparticles loaded with siRNA. J. Control. Release 157 (1), 141–148. https://doi.org/10.1016/j.jconrel.2011.08.011.

Judge, A.D., Sood, V., Shaw, J.R., Fang, D., McClintock, K., MacLachlan, I., 2005. Sequence-dependent stimulation of the mammalian innate immune response by synthetic siRNA. Nat. Biotechnol. 23 (4), 457–462. https://doi.org/10.1038/nbt1081.

Kanasty, R., Dorkin, J.R., Vegas, A., Anderson, D., 2013. Delivery materials for siRNA therapeutics. Nat. Mater. 12 (11), 967–977. https://doi.org/10.1038/nmat3765.

Kany, S., Vollrath, J.T., Relja, B., 2019. Cytokines in inflammatory disease. Int. J. Mol. Sci. 20 (23), 6008. https://doi.org/10.3390/ijms20236008.

Kedmi, R., Ben-Arie, N., Peer, D., 2010. The systemic toxicity of positively charged lipid nanoparticles and the role of Toll-like receptor 4 in immune activation. Biomaterials 31. https://doi.org/10.1016/j.biomaterials.2010.05.027.

Kim, J.Y., Choung, S., Lee, E.J., Kim, Y.J., Choi, Y.C., 2007. Immune activation by siRNA/liposome complexes in mice is sequence- independent: lack of a role for toll-like receptor 3 signaling. Mol. Cell 31 (26), 6867–6875.

Kim, S., Oh, W.K., Jeong, Y.S., Hong, J.Y., Cho, B.R., Hahn, J.S., Jang, J., 2011. Cytotoxicity of, and innate immune response to, size-controlled polypyrrole nanoparticles in mammalian cells. Biomaterials. 32 (9), 2342–2350. https://doi.org/10.1016/j.biomaterials.2010.11.080.

Lawson, N.D., Krause, D.S., Berliner, N., 1998. Normal neutrophil differentiation and secondary granule gene expression in the EML and MPRO cell lines. Exp. Hematol. 26 (12), 1178–1185.

Lechanteur, A., Sanna, V., Duchemin, A., Evrard, B., Mottet, D., Piel, G., 2018. Cationic liposomes carrying siRNA: Impact of lipid composition on physicochemical properties, cytotoxicity and endosomal escape. Nanomaterials. 8 (5), 270. https://doi.org/10.3390/nano8050270.

Lonez, C., Bessodes, M., Scherman, D., Vandenbranden, M., Escriou, V., Ruysschaert, J. M., 2014. Cationic lipid nanocarriers activate Toll-like receptor 2 and NLRP3 inflammasome pathways. Nanomedicine. 10 (4), 775–782. https://doi.org/10.1016/j.nano.2013.12.003.

Lv, H., Zhang, S., Wang, B., Cui, S., Yan, J., 2006. Toxicity of cationic lipids and cationic polymers in gene delivery. J. Control. Release 114 (1), 100–109. https://doi.org/10.1016/j.jconrel.2006.04.014.

Ma, Z., Li, J., He, F., Wilson, A., Pitt, B., Li, S., 2005. Cationic lipids enhance siRNA-mediated interferon response in mice. Biochem. Biophys. Res. Commun. 330 (3), 755–759. https://doi.org/10.1016/j.bbrc.2005.03.041.

Mansury, D., Ghazvini, K., Jamehdar, S.A., Badiee, A., Tafaghodi, M., Nikpoor, A.R., Amini, Y., Jaafari, M.R., 2019. Increasing cellular immune response in liposomal formulations of DOTAP encapsulated by fusion protein Hspx, PPE44, and Esxv, as a potential tuberculosis vaccine candidate. Rep. Biochem. Mol. Biol. 7 (2), 156.

Mendonça, M.C.P., Radaic, A., Garcia-Fossa, F., da Cruz-Höfling, M.A., Vinolo, M.A.R., de Jesus, M.B., 2020. The in vivo toxicological profile of cationic solid lipid nanoparticles. Drug Deliv. Transl. Res. 10, 34–42. https://doi.org/10.1007/s13346-019-00657-8.

Moon, J.S., Lee, S.H., Han, Song Hee, Kim, E.J., Cho, H., Lee, W., Kim, M.K., Kim, T.E., Park, H.J., Rhee, J.K., Kim, S.J., Cho, S.W., Han, Seung Hyun, Oh, J.W., 2016. Inhibition of hepatitis C virus in mouse models by lipidoid nanoparticle-mediated systemic delivery of siRNA against PRK2. Nanomedicine. 12 (6), 1489–1498. https://doi.org/10.1016/j.nano.2016.02.015.

Nazar, M.F., Murtaza, S., 2014. Physicochemical investigation and spectral properties of Sunset Yellow dye in cetyltrimethylammonium bromide micellar solution under different pH conditions. Color. Technol. 130 (3), 191–199. https://doi.org/10.1111/cote.12085.

Okamoto, A., Asai, T., Kato, H., Ando, H., Minamino, T., Mekada, E., Oku, N., 2014. Antibody-modified lipid nanoparticles for selective delivery of siRNA to tumors expressing membrane-anchored form of HB-EGF. Biochem. Biophys. Res. Commun. 449 (4), 460–465. https://doi.org/10.1016/j.bbrc.2014.05.043.

Pinnaduwage, P., Schmitt, L., Huang, L., 1989. Use of a quaternary ammonium detergent in liposome mediated DNA transfection of mouse L-cells. BBA – Biomembranes 985 (1), 33–37. https://doi.org/10.1016/0005-2736(89)90099-0.

Robbins, M., Judge, A., MacLachlan, I., 2009. SiRNA and innate immunity. Oligonucleotides. 19 (2), 89–102. https://doi.org/10.1089/oli.2009.0180.

Rungta, R.L., Choi, H.B., Lin, P.J.C., Ko, R.W.Y., Ashby, D., Nair, J., Manoharan, M., Cullis, P.R., MacVicar, B.A., 2013. Lipid nanoparticle delivery of sirna to silence neuronal gene expression in the brain. Mol. Ther. Nucleic Acids. 2 (12), e136 https://doi.org/10.1038/mtna.2013.65.

Sato, Y., Matsui, H., Yamamoto, N., Sato, R., Munakata, T., Kohara, M., Harashima, H., 2017. Highly specific delivery of siRNA to hepatocytes circumvents endothelial cell-mediated lipid nanoparticle-associated toxicity leading to the safe and efficacious decrease in the hepatitis B virus. J. Control. Release 266, 216–225. https://doi.org/10.1016/j.jconrel.2017.09.044.

Silva, A.M., Martins-Gomes, C., Coutinho, T.E., Fangueiro, J.F., Sanchez-Lopez, E., Pashirova, T.N., Andreani, T., Souto, E.B., 2019. Soft cationic nanoparticles for drug delivery: production and cytotoxicity of solid lipid nanoparticles (SLNs). Appl. Sci. 9 (20), 4438. https://doi.org/10.3390/app9204438.

Soenen, S.J.H., Brisson, A.R., De Cuyper, M., 2009. Addressing the problem of cationic lipid-mediated toxicity: the magnetoliposome model. Biomaterials. 30 (22), 3691–3701. https://doi.org/10.1016/j.biomaterials.2009.03.040.

Tada, R., Hidaka, A., Iwase, N., Takahashi, S., Yamakita, Y., Iwata, T., Muto, S., Sato, E., Takayama, N., Honjo, E., Kiyono, H., Kunisawa, J., Aramaki, Y., Boyaka, P.N., 2015. Intranasal immunization with dotap cationic liposomes combined with DC-cholesterol induces potent antigen-specific mucosal and systemic immune responses in mice. PLoS One 10 (10), e0139785. https://doi.org/10.1371/journal.pone.0139785.

Tan, Y., Huang, L., 2002. Overcoming the inflammatory toxicity of cationic gene vectors. J. Drug Target. 10 (2), 153–160. https://doi.org/10.1080/106118602900167 57.

Tang, F., Hughes, J.A., 1999. Synthesis of a single-tailed cationic lipid and investigation of its transfection. J. Control. Release 62 (3), 345–358. https://doi.org/10.1016/S0168-3659(99)00158-3.

Wei, X., Shao, B., He, Z., Ye, T., Luo, M., Sang, Y., Liang, X., Wang, W., Luo, S., Yang, S., Zhang, S., Gong, C., Gou, M., Deng, H., Zhao, Y., Yang, H., Deng, S., Zhao, C., Yang, L., Qian, Z., Li, J., Sun, X., Han, J., Jiang, C., Wu, M., Zhang, Z., 2015. Cationic nanocarriers induce cell necrosis through impairment of Na+/K+-ATPase and cause subsequent inflammatory response. Cell Res. 25 (2), 237–253. https://doi.org/10.1038/cr.2015.9.

Yamamoto, Y., Lin, P.J.C., Beraldi, E., Zhang, F., Kawai, Y., Leong, J., Katsumi, H., Fazli, L., Fraser, R., Cullis, P.R., Gleave, M.E., 2015. siRNA lipid nanoparticle potently silences clusterin and delays progression when combined with androgen receptor cotargeting in enzalutamide-resistant prostate cancer. Clin. Cancer Res. 21 (21), 4845–4855. https://doi.org/10.1158/1078-0432.CCR-15-0866.

Zhu, S., Niu, M., O'Mary, H., Cui, Z., 2013a. Targeting of tumor-associated macrophages made possible by PEG-sheddable mannose-modified nanoparticles. Mol. Pharm. 10 (9), 3525–3530. https://doi.org/10.1021/mp400216r.

Zhu, S., Wonganan, P., Lansakara-P, D.S., O'Mary, H.L., Li, Y., Cui, Z., 2013b. The effect of the acid-sensitivity of 4-(N)-stearoyl gemcitabine-loaded micelles on drug resistance caused by RRM1 overexpression. Biomaterials 34 (9), 2327–2339. https://doi.org/10.1016/j.biomaterials.2012.11.053.

Zhang, L., Wang, C.C., 2014. Inflammatory response of macrophages in infection. Hepatob. Pancreatic Dis. Int. 13 (2), 138–152. https://doi.org/10.1016/s1499-3872(14)60024-2.

Zhao, Y., Gao, H., He, J., Jiang, C., Lu, J., Zhang, W., Yang, H., Liu, J., 2018. Co-delivery of LOX-1 siRNA and statin to endothelial cells and macrophages in the atherosclerotic lesions by a dual-targeting core-shell nanoplatform: a dual cell therapy to regress plaques. J. Control. Release 283, 241–260. https://doi.org/10.1016/j.jconrel.2018.05.041.

Zhu, Y., Meng, Y., Zhao, Y., Zhu, J., Xu, H., Zhang, E., Shi, L., Du, L., Liu, G., Zhang, C., Xu, X., Kang, X., Zhen, Y., Zhang, S., 2019. Toxicological exploration of peptide-based cationic liposomes in siRNA delivery. Colloids Surf. B: Biointerfaces 179, 66–76. https://doi.org/10.1016/j.colsurfb.2019.03.052.